

Supporting information

Locally regulating Li⁺ distribution on electrode surface with Li-Sn alloying nanoparticles for stable lithium metal anodes

Jianzong Man *^a, Wenlong Liu ^b, Xiaodong Sun ^b, Juncai Sun *^b

^a Shandong Provincial Key Laboratory of Chemical Energy Storage and New Battery Technology, Liaocheng University, Liaocheng, 252000, China

^b Institute of Materials and Technology, Dalian Maritime University, Dalian, 116026, China

* Corresponding author:

manjianzong@lcu.edu.cn (J. Man); sunjc@dlmu.edu.cn (J. Sun)

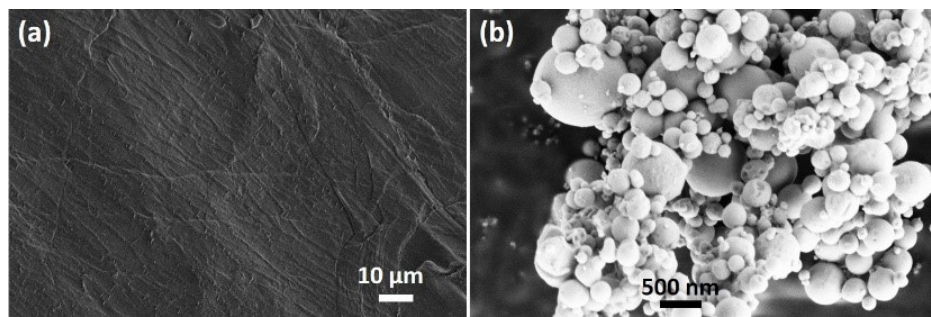


Fig. S1 The SEM images of (a) bare Li and (b) Sn powders.

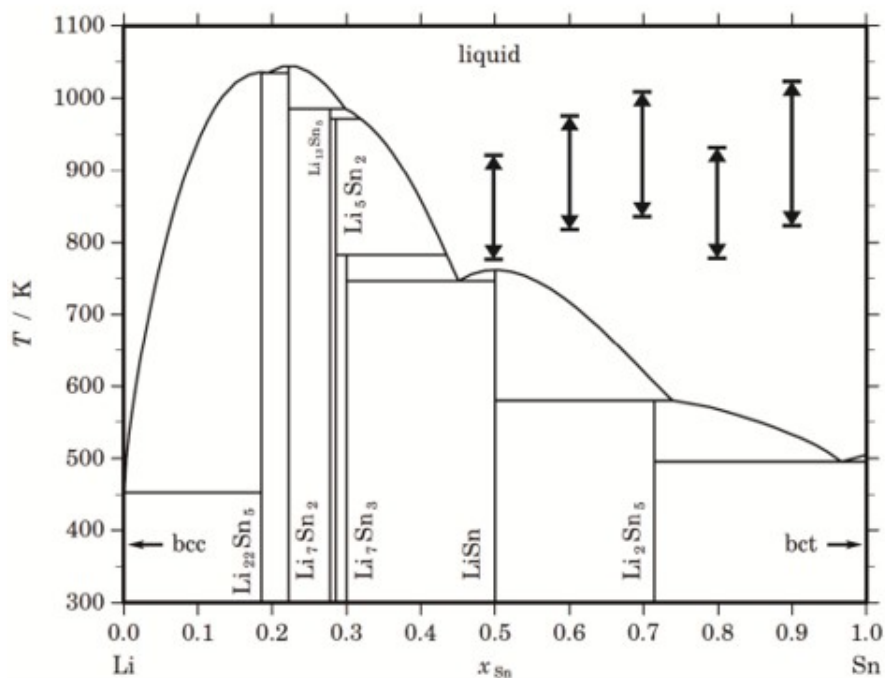


Fig. S2 The binary phase diagram of Li-Sn.

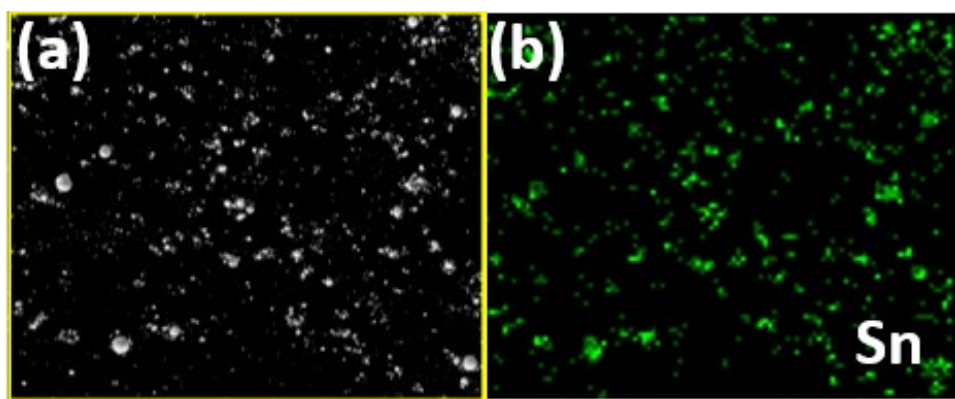


Fig. S3 The elemental distribution of Sn on the surface of Li-Sn anode.

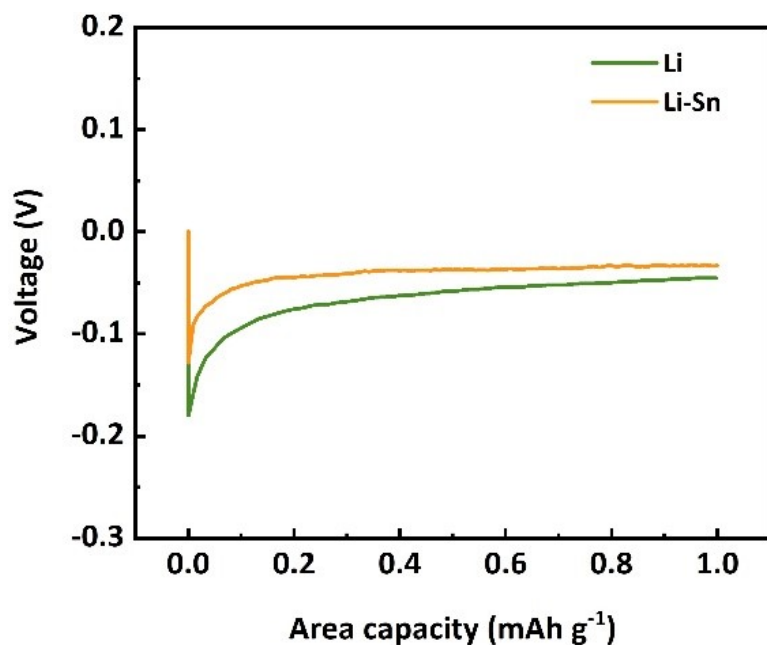


Fig. S4 Comparison of Li nucleation overpotential on the bare Li and Li-Sn anode.

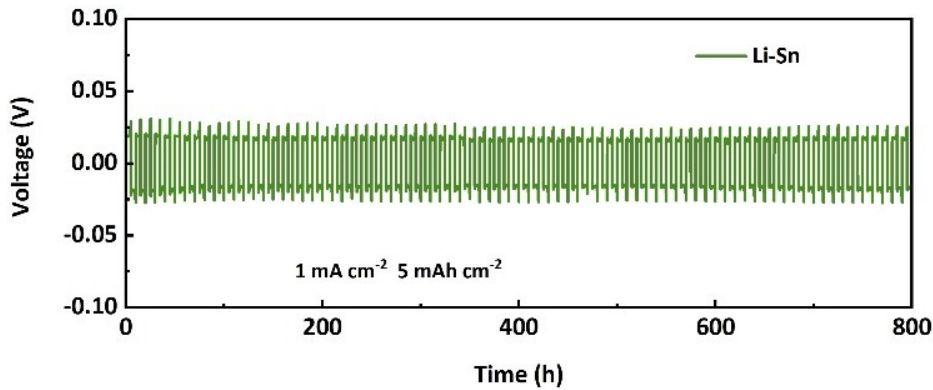


Fig. S5 The cycling performance of Li-Sn symmetrical cell with the plating/stripping capacity of 5 mAh cm^{-2} at the current density of 1 mA cm^{-2} .

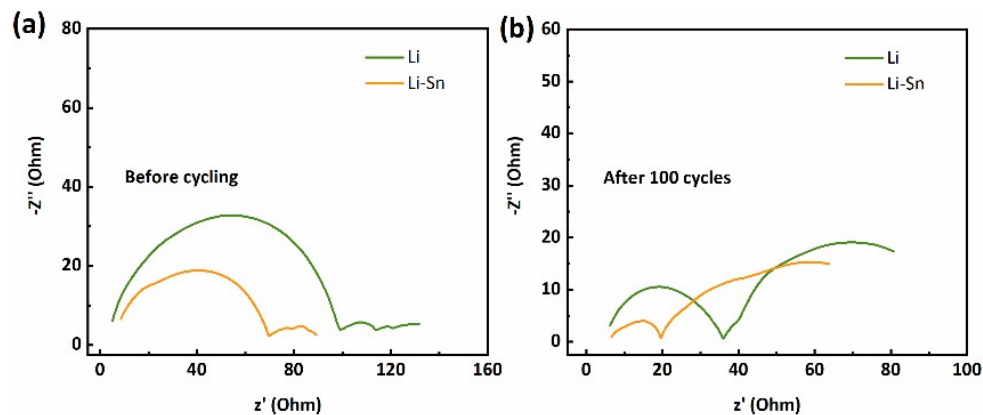


Fig. S6 Comparison of impedance of bare Li and Li-Sn symmetrical cells before cycling and after 100 cycles.

Table S1 Comparison of electrochemical performance of similar configuration of anode.

Li-M alloy anode	Modification method	Current density-capacity (mA cm ⁻² -mAh cm ⁻²)	Hysteresis voltage (mV)	Cycling time (h)	Reference
Li@NFZO	Li melting infusion	1-1	57	700	[1]
Li-LiAl	Li-Al thermal melting	1-1	15	1100	[2]
Li@Li-Zn	Depositing Zn on Cu foam- electrochemical deposition	1-1	23	400	[3]
Li@CuSn	Electroless Sn plating- electrochemical deposition	1-1	~20	800	[4]
CP/Sn/SnO ₂ @Li	Heat treatment (SnO ₂ , Li)	1-1	~25	800	[5]
Li-Mg alloy	Melting-spontaneous reaction	1-1	23	1000	[6]
Sn-Li scaffold	Electrodeposition	1-1	21.3	750	[7]
Li-Sn	Rolling	1-1	10	1200	This work
		1-5	20	800	

Table S2 Simulation parameters of impedance for bare Li and Li-Sn symmetrical cells before and after cycling.

Electrode	Before cycling		After 100 cycles	
	R _{SEI} (Ω)	R _{ct} (Ω)	R _{SEI} (Ω)	R _{ct} (Ω)
Li	93.4	14.2	30.5	68.1
Li-Sn	60.7	9.3	13.2	59.6

References:

- [1] J. Jia, Z. Tang, Z. Guo, H. Xu, H. Hu, S. Li, 3D composite lithium metal anode with pre-fabricated LiZn via reactive wetting, *Chem. Commun.*, 56 (2020) 4248-4251.
- [2] H. Zhuang, P. Zhao, G. Li, Y. Xu, X. Jia, Li-LiAl alloy composite with memory effect as high-performance lithium metal anode, *J. Power Sources*, 455 (2020) 227977.
- [3] Y. Ye, Y. Liu, J. Wu, Y. Yang, Lithiophilic Li-Zn alloy modified 3D Cu foam for dendrite-free lithium metal anode, *J. Power Sources*, 472 (2020) 228520.
- [4] Z. Luo, C. Liu, Y. Tian, Y. Zhang, Y. Jiang, J. Hu, H. Hou, G. Zou, X. Ji, Dendrite-free lithium metal anode with lithiophilic interphase from hierarchical frameworks by tuned nucleation, *Energy Storage Materials*, 27 (2020) 124-132.
- [5] L. Tan, S. Feng, X. Li, Z. Wang, W. Peng, T. Liu, G. Yan, L. Li, F. Wu, J. Wang, Oxygen-induced lithiophilicity of tin-based framework toward highly stable lithium metal anode, *Chem. Eng. J.*, 394 (2020) 124848.
- [6] K. Peng, Z. Chen, X. Zhao, K. Shi, C. Zhu, X. Yan, Dual-Conductive Li alloy composite anode constructed by a synergetic Conversion-Alloying reaction with LiMgPO₄, *Chem. Eng. J.*, 439 (2022) 135705.
- [7] L. Ren, X. Cao, Y. Wang, M. Zhou, W. Liu, H. Xu, H. Zhou, X. Sun, 3D porous and li-rich sn-li alloy scaffold with mixed Ionic-Electronic conductivity for Dendrite-Free lithium metal anodes, *J. Alloy Compd.*, (2023) 169362.